Time-delayed Decentralized $\mathcal{H}_\infty$ Controller Design for Civil Structures: a Homotopy Method through Linear Matrix Inequalities

Yang Wang, Kincho H. Law, and Sanjay Lall

***Abstract*—Traditional structural feedback control systems are centralized systems. The applications of these systems to large scale structures usually encounter a number of difficulties regarding system reliability, cost, and feedback latency. Decentralized control strategies offer promising alternatives that can address some of these difficulties. When making control decisions, decentralized controllers may only require data from sensors located in the neighborhood of a control device. Control decentralization lowers the demand on communication range in the sensing and control network, reduces feedback latency, and removes the risk associated with a centralized controller where single-point failure can paralyze the entire control system.**

This paper presents a time-delayed decentralized structural control strategy that aims to minimize the $\mathcal{H}_\infty$ norm of the closed-loop system. Feedback time delay is included in the formulation for the decentralized controller design, which employs a homotopy method through linear matrix inequalities (LMI). Corresponding to certain decentralized feedback patterns, the homotopy method gradually degenerates a centralized control design into a decentralized control scheme. At each homotopy step, LMI constraints are satisfied to guarantee the performance requirement for the closed-loop $\mathcal{H}_\infty$ norm. The proposed algorithm is validated through numerical simulations with an example structure.

I. Introduction

Over the last three decades, significant research has been conducted in structural control technologies that aim to reduce excessive structural vibrations during earthquakes and typhoons [1, 2]. Structural control systems can be categorized into three major types: (a) passive control, (b) active control, and (c) semi-active control. Passive control systems, e.g. base isolators, entail the use of passive energy dissipation devices to reduce the response of a structure. Active control systems utilize actuators with high force capacities, such as active mass dampers, for direct application of control forces. In a semi-active control system, control devices with adjustable properties are used for indirect application of control forces. Examples of semi-active control devices include active variable stiffness (AVS) devices, semi-active hydraulic dampers (SHD), electrorheological (ER) dampers, and magnetorheological (MR) dampers, etc.

In both active and semi-active control systems, sensors are deployed in the structure to collect structural response data during dynamic excitations. Sensor data is sent to the controllers that determine appropriate control forces and deliver commands to structural control devices. The control devices then generate forces intended to mitigate undesirable structural vibrations. In traditional feedback control systems, coaxial wires are normally used to provide communication links between sensors, controllers and control devices. The emergence of wireless communication and embedded computing technologies offers possible alternatives for the feedback communication links and decision making hardware in a structural control system [3, 4]. Incorporated with embedded computing power, "smart" wireless sensors can assume the responsibilities of both sensors and controllers. They can not only exchange sensor data with other neighboring nodes, but also make informed control decisions and command structural control devices. The adoption of wireless communication and embedded computing has the potential to significantly reduce the cost and increase the architecture flexibility of a feedback structural control system.

In previous research, a prototype wireless sensing and control system has been developed and its application to real-time feedback structural control has been explored in a laboratory setting [3]. When replacing cables with wireless communication channels, issues such as coordination of sensing and control nodes, communication range, feedback time delay and potential data loss need to be examined. For example, time delay due to wireless communication will cause degradation to the performance of a feedback control system [5]. In general, the issue of communication time delay is common for any large-scale feedback control systems, regardless of using cabled or wireless communication. To resolve some of the difficulties with centralized control, decentralized control strategies can be adopted [6]. For decentralized control, a large-scale control system is divided into a collection of smaller and distributed sub-systems. In each subsystem, decentralized controllers rely only on local and neighboring sensor data to make control decisions. For both cabled and wireless control networks, decentralization offers reduced use of communication channel, higher control sampling rates, shorter feedback time delay, and lower requirements on communication range. Decentralization also removes the risk associated with a centralized controller being the single vulnerable point, whose failure would paralyze the

Manuscript received September 15, 2008.

Y. Wang is at the School of Civil and Environmental Engineering, Georgia Institute of Technology, Atlanta, GA 30332 USA (phone: 1-404-894-1851; fax: 1-404-894-2278; e-mail: yang.wang@ce.gatech.edu).

K. H. Law is at the Department of Civil and Environmental Engineering, Stanford University, Stanford, CA 94305 USA (e-mail: law@stanford.edu).

S. Lall is at the Department of Aeronautics and Astronautics, Stanford University, Stanford, CA 94305 USA (e-mail: lall@stanford.edu).

entire control system. On the other hand, because each decentralized controller only has local and neighboring sensor data available for control decisions, decentralized control systems may only achieve sub-optimal control performance when compared to centralized systems. Therefore, decentralized controllers need to be designed with special consideration.

To ensure satisfactory control performance, decentralized structural controller design based on the linear quadratic regulator (LQR) optimization criteria has been studied [3]. The design provides static output feedback controllers which consider the effect of feedback time delay. This paper explores a different control methodology, namely the $\mathcal{H}_\infty$ control theory that can offer excellent control performance when "worst-case" external disturbances are encountered. Centralized $\mathcal{H}_\infty$ controller design in the continuous-time domain for structural control has been studied by researchers [7-10]. Their work illustrates the feasibility and effectiveness of centralized $\mathcal{H}_\infty$ control for civil structures. For example, it has been shown that $\mathcal{H}_\infty$ control design may achieve excellent performance in attenuating transient vibrations of structures [11]. However, decentralized $\mathcal{H}_\infty$ controller design has rarely been explored in structural control.

$\mathcal{H}_\infty$ controller design can be conveniently formulated using linear matrix inequalities (LMI) [12]. For an optimization problem with LMI constraints, sparsity patterns can be easily applied to the matrix variables. This property offers great convenience for designing decentralized controllers where sparsity patterns in the parametric controller matrices can represent decentralized information feedback. Preliminary research on decentralized $\mathcal{H}_\infty$ controller design, which is based on static state feedback, has been reported [13]. The work, however, did not consider feedback time delay in the controller design. Since time delay inevitably exists in a practical structural control system, the inability to consider time delay during controller design may result in significant performance degradation. Because the previous formulation for the decentralized $\mathcal{H}_\infty$ controller design cannot be easily extended to provide controllers that can effectively consider feedback time delay, or controllers that do not require state feedback, a new approach is pursued in this work.

This paper describes a new decentralized $\mathcal{H}_\infty$ structural controller design that offers dynamic output feedback controllers. The control problem is formulated in discrete-time domain so that feedback time delay can be effectively considered. A homotopy method for designing decentralized $\mathcal{H}_\infty$ controllers in continuous-time domain, which was described by Zhai, *et al.* [14], is adapted for this work. The method gradually degenerates a centralized controller into a decentralized scheme that corresponds to certain decentralized feedback patterns. LMI constraints describing the closed-loop $\mathcal{H}_\infty$ norm performance are guaranteed at each homotopy step. This paper first describes the formulation of multiple dynamical systems involved in controller design. The homotopy method that computes decentralized $\mathcal{H}_\infty$ controllers is then described. Numerical simulations with an example structure are conducted to validate the performance of the proposed controller design.

II. Problem Formulation

For a lumped-mass structural model with n degrees-of-freedom (DOF) and instrumented with n_u control devices, the equations of motion can be formulated as:

$$\mathbf{M}\ddot{\mathbf{q}}(t)+\mathbf{C}\dot{\mathbf{q}}(t)+\mathbf{K}\mathbf{q}(t)=\mathbf{T}_{\mathbf{w}_1}\mathbf{w}_1(t)+\mathbf{T}_\mathbf{u}\mathbf{u}(t) \tag{1}$$

where $\mathbf{q}(t) \in \mathbb{R}^{n\times 1}$ is the displacement vector relative to the ground; $\mathbf{M}$, $\mathbf{C}$, $\mathbf{K} \in \mathbb{R}^{n\times n}$ are the mass, damping, and stiffness matrices, respectively; $\mathbf{w}_1(t) \in \mathbb{R}^{n_{w1}\times 1}$ and $\mathbf{u}(t) \in \mathbb{R}^{n_u\times 1}$ are the external excitation vector and control force vector, respectively; and $\mathbf{T}_{\mathbf{w}1} \in \mathbb{R}^{n\times n_{w1}}$ and $\mathbf{T}_\mathbf{u} \in \mathbb{R}^{n\times n_u}$ are the external excitation and control force location matrices, respectively.

Without any loss of generality, the discussion is based on a 2-D shear-frame structure subject to unidirectional ground excitation. The control formulation can be easily extended to 3-D structural models. For the example structure shown in Fig. 1, it is assumed that the external excitation $\mathbf{w}_1(t)$ is a scalar (n_{w1} = 1), *i.e.* the ground acceleration history $\ddot{q}_g(t)$. The spatial load pattern $\mathbf{T}_{\mathbf{w}1}$ is equal to $-\mathbf{M}\{\mathbf{1}\}_{n\times 1}$. Entries in $\mathbf{u}(t)$ are defined as the control forces between neighboring floors. For the three-story structure, if a positive control force is defined to be moving the floor above the control device towards the left direction, and moving the floor below the control device towards the right direction (directions of forces acting on the floors are shown in Fig. 1), the control force location matrix $\mathbf{T}_\mathbf{u}$ is determined as:

$$\mathbf{T}_\mathbf{u}=\begin{bmatrix}-1 & 1 & 0\\ 0 & -1 & 1\\ 0 & 0 & -1\end{bmatrix} \tag{2}$$

The state-space system can be formulated as:

$$\dot{\mathbf{x}}_I(t)=\mathbf{A}_I\mathbf{x}_I(t)+\mathbf{E}_I\mathbf{w}_1(t)+\mathbf{B}_I\mathbf{u}(t) \tag{3}$$

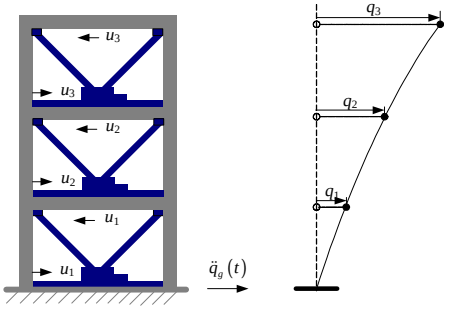

Fig. 1. A three-story controlled structure excited by unidirectional ground motion.

where $\mathbf{x}_I(t) = \left[\mathbf{q}(t); \dot{\mathbf{q}}(t)\right] \in \mathbb{R}^{2n\times 1}$ is the state vector; $\mathbf{A}_I \in \mathbb{R}^{2n\times 2n}$, $\mathbf{E}_I \in \mathbb{R}^{2n\times n_{w1}}$, and $\mathbf{B}_I \in \mathbb{R}^{2n\times n_u}$ are the system, excitation influence, and control influence matrices, respectively [15].

To facilitate the derivation for decentralized control, a linear transformation to the state vector is performed. The transformed state vector $\mathbf{x}_{II}(t) \in \mathbb{R}^{2n\times 1}$, with the displacement and velocity terms at the same story being concatenated together, is denoted as:

$$\mathbf{x}_{II}(t) = [q_1(t) \quad \dot{q}_1(t) \quad q_2(t) \quad \dot{q}_2(t) \quad \cdots \quad q_n(t) \quad \dot{q}_n(t)]^{\mathrm{T}} \tag{4}$$

To obtain the transformed state vector $\mathbf{x}_{II}(t)$, a linear transformation matrix $\mathbf{\Gamma}$ is defined to shuffle the entries in the original state vector $\mathbf{x}_I(t)$:

$$\mathbf{x}_{II}(t) = \mathbf{\Gamma}\mathbf{x}_I(t) \tag{5}$$

Substituting $\mathbf{x}_I(t) = \mathbf{\Gamma}^{-1}\mathbf{x}_{II}(t)$ into (3), and left-multiplying the equation with $\mathbf{\Gamma}$, the state space representation using the transformed state vector becomes:

$$\dot{\mathbf{x}}_{II}(t) = \mathbf{A}_{II}\mathbf{x}_{II}(t) + \mathbf{E}_{II}\mathbf{w}_1(t) + \mathbf{B}_{II}\mathbf{u}(t) \tag{6}$$

where $\mathbf{A}_{II} = \mathbf{\Gamma}\mathbf{A}_I\mathbf{\Gamma}^{-1}$, $\mathbf{E}_{II} = \mathbf{\Gamma}\mathbf{E}_I$ and $\mathbf{B}_{II} = \mathbf{\Gamma}\mathbf{B}_I$. The system output vector $\mathbf{z}(t) \in \mathbb{R}^{n_z\times 1}$ is defined as:

$$\mathbf{z}(t) = \mathbf{C}_\mathbf{z}\mathbf{x}_{II}(t) + \mathbf{F}_\mathbf{z}\mathbf{w}_1(t) + \mathbf{D}_\mathbf{z}\mathbf{u}(t) \tag{7}$$

Similarly, the sensor measurement vector $\mathbf{m}(t) \in \mathbb{R}^{n_m\times 1}$ can be defined in a general form as:

$$\mathbf{m}(t) = \mathbf{C}_\mathbf{m}\mathbf{x}_{II}(t) + \mathbf{F}_\mathbf{m}\mathbf{w}_1(t) + \mathbf{D}_\mathbf{m}\mathbf{u}(t) \tag{8}$$

Using zero-order hold, the continuous-time dynamics in (6) can be discretized using a sampling period Δt. The complete discrete-time system can be summarized as:

$$\begin{cases} \mathbf{x}_S[k+1] = \mathbf{A}_\mathbf{d}\mathbf{x}_S[k] + \mathbf{E}_\mathbf{d}\mathbf{w}_1[k] + \mathbf{B}_\mathbf{d}\mathbf{u}[k] \\ \mathbf{z}[k] = \mathbf{C}_\mathbf{z}\mathbf{x}_S[k] + \mathbf{F}_\mathbf{z}\mathbf{w}_1[k] + \mathbf{D}_\mathbf{z}\mathbf{u}[k] \\ \mathbf{m}[k] = \mathbf{C}_\mathbf{m}\mathbf{x}_S[k] + \mathbf{F}_\mathbf{m}\mathbf{w}_1[k] + \mathbf{D}_\mathbf{m}\mathbf{u}[k] \end{cases} \tag{9}$$

where k represents the discrete time step, and the subscript "d" denotes the corresponding variables expressed in discrete-time domain.

In this work, it is assumed that one step of time delay exists for the sensor measurement signal $\mathbf{m}[k]$, *i.e.* the feedback time delay is equal to one sampling period Δt. This is typically encountered in a wireless feedback structural control system, where the dominant part of feedback delay is the communication delay [3]. The sensor noise vector is denoted as $\mathbf{w}_2[k] \in \mathbb{R}^{n_{w2}\times 1}$. To describe one-step time delay and sensor noises, a simple discrete-time system can be defined as:

$$\begin{cases} \mathbf{x}_{TD}[k+1] = \mathbf{A}_{TD}\mathbf{x}_{TD}[k] + \mathbf{B}_{TD}\begin{bmatrix}\mathbf{m}[k] \\ \mathbf{w}_2[k]\end{bmatrix} \\ \mathbf{y}[k] = \mathbf{C}_{TD}\mathbf{x}_{TD}[k] + \mathbf{D}_{TD}\begin{bmatrix}\mathbf{m}[k] \\ \mathbf{w}_2[k]\end{bmatrix} \end{cases} \tag{10}$$

where

$$\mathbf{A}_{TD} = \mathbf{0},\ \mathbf{B}_{TD} = [\mathbf{I} \quad \mathbf{0}],\ \mathbf{C}_{TD} = \mathbf{I},\ \mathbf{D}_{TD} = \begin{bmatrix}\mathbf{0} & s_{w_2}\mathbf{I}\end{bmatrix} \tag{11}$$

The input to this system is the original measurement signal $\mathbf{m}[k]$ and the sensor noise $\mathbf{w}_2[k]$, the output of the system is the delayed noisy signal $\mathbf{y}[k]$, which is the feedback signal to be used for control decisions. The formulation can be easily adapted and extended to model multiple steps of time delay, as well as different steps of time delay associated with different sensing channels. Parameter s_{w_2} is the scaling factor representing sensor noise level. For simplicity, a single scaling factor is assumed for all sensor noises.

This study is interested in decentralized schemes where the delayed measurement signal $\mathbf{y}[k]$ is fed back to the controllers. For a clear description of the decentralized control strategy, a simple three-story example structure is adopted herein. Nevertheless, the formulation is general-purpose and applies to larger-scale structures, where the benefit of decentralization can be much more significant. Fig. 2 illustrates two decentralized feedback patterns for the three-story structure. It is assumed that at each floor i (i = 1, 2, or 3), two measurement signals, $y_{2i\text{-}1}[k]$ and $y_{2i}[k]$, are acquired by sensors at that floor. In Fig. 2(a), the feedback pattern is defined such that when making the decision for control device u_i, only measurement signals from the i-th floor are needed. Fig. 2(b) illustrates a partially decentralized feedback pattern with information overlapping. In this case, sensor measurements from neighboring floors (floor) are also available for making the control decision for control device u_i.

To represent the information overlapping shown in Fig. 2(b), one delayed measurement signal is repeated as multiple entries in $\mathbf{y}[k]$. Redundant rows are added into the definition of $\mathbf{y}[k]$ in (10); the entries in $\mathbf{y}[k]$ are then aggregated according to different information groups. For example, for the feedback pattern illustrated in Fig. 2(b), the delayed sensor measurement signal $\mathbf{y}[k]$ is replaced by the new vector $\mathbf{y}_{repeat}$ defined in Fig. 3. The entries are aggregated into three groups, which correspond to the sensor measurements required by three control devices. This process is to facilitate the design of uncoupled decentralized controllers.

The dynamical system that describes time delay, sensor noises, and signal repeating is connected with the structural system in (9) to constitute the open-loop system depicted in Fig. 4. The number of state variables in the open-loop system is equal to the total number of state variables in the structural system and the time-delay system, *i.e.* $n_{OL} = 2n + n_{TD}$. Combining the structural system and the time-delay system, the complete open-loop system is denoted as follows:

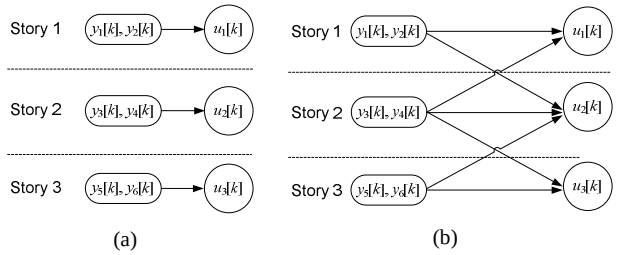

Fig. 2. Decentralized feedback patterns: (a) fully decentralized with no information overlapping; (b) partially decentralized with information overlapping.

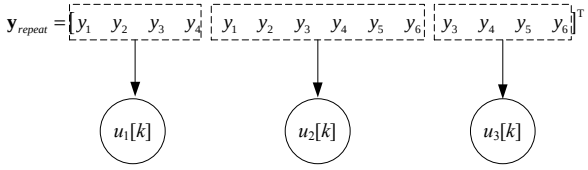

Fig. 3. Redundant entries are used to represent signal repeating for decentralized feedback with information overlapping.

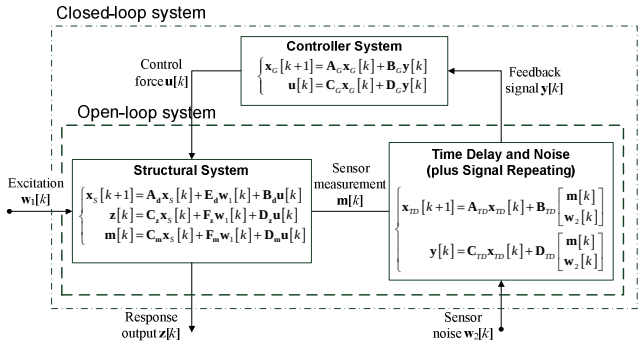

Fig. 4. Diagram of the structural control system.

$$\begin{cases} \mathbf{x}[k+1] = \mathbf{A}\mathbf{x}[k] + \mathbf{B}_1\mathbf{w}[k] + \mathbf{B}_2\mathbf{u}[k] \\ \mathbf{z}[k] = \mathbf{C}_1\mathbf{x}[k] + \mathbf{D}_{11}\mathbf{w}[k] + \mathbf{D}_{12}\mathbf{u}[k] \\ \mathbf{y}[k] = \mathbf{C}_2\mathbf{x}[k] + \mathbf{D}_{21}\mathbf{w}[k] + \mathbf{D}_{22}\mathbf{u}[k] \end{cases} \tag{12}$$

where $\mathbf{w}[k]$ contains both the external excitation $\mathbf{w}_1[k]$ and the sensor noise $\mathbf{w}_2[k]$:

$$\mathbf{w}[k] = \begin{Bmatrix} \mathbf{w}_1[k] \\ \mathbf{w}_2[k] \end{Bmatrix} \tag{13}$$

The control objective is to design an effective feedback controller for the open-loop system with different feedback patterns. The controller takes the feedback signal $\mathbf{y}[k]$ as input, and outputs the control force vector $\mathbf{u}[k]$:

$$\begin{cases} \mathbf{x}_G[k+1] = \mathbf{A}_G\mathbf{x}_G[k] + \mathbf{B}_G\mathbf{y}[k] \\ \mathbf{u}[k] = \mathbf{C}_G\mathbf{x}_G[k] + \mathbf{D}_G\mathbf{y}[k] \end{cases} \tag{14}$$

It is assumed that the controller has same number of states as the open-loop system, *i.e.* $\mathbf{A}_G \in \mathbb{R}^{n_G \times n_G}$ and $n_G = n_{OL}$. For convenience, a matrix variable $\mathbf{G} \in \mathbb{R}^{(n_G+n_u)\times(n_G+n_y)}$ is defined to contain all controller parametric matrices:

$$\mathbf{G} = \begin{bmatrix} \mathbf{A}_G & \mathbf{B}_G \\ \mathbf{C}_G & \mathbf{D}_G \end{bmatrix} \tag{15}$$

III. Decentralized Discrete-time $\mathcal{H}_\infty$ Controller Design

For a decentralized controller design, the decentralized feedback can be represented by sparsity patterns in the controller matrices $\mathbf{A}_G$, $\mathbf{B}_G$, $\mathbf{C}_G$ and $\mathbf{D}_G$. For this purpose, entries in the feedback signal $\mathbf{y}[k]$ and the control force $\mathbf{u}[k]$ are divided into N groups. While making control decisions for one group of control force entries, only one group of corresponding feedback signals is needed. Block-diagonal patterns are assigned to controller matrices in order to represent a decentralized control architecture that includes decentralized controllers $\mathbf{G}_I$, $\mathbf{G}_{II}$, …, and $\mathbf{G}_N$:

$$\begin{aligned} &\mathbf{A}_G = diag\left(\mathbf{A}_{G_I}, \mathbf{A}_{G_{II}}, \cdots, \mathbf{A}_{G_N}\right), \mathbf{B}_G = diag\left(\mathbf{B}_{G_I}, \mathbf{B}_{G_{II}}, \cdots, \mathbf{B}_{G_N}\right), \\ &\mathbf{C}_G = diag\left(\mathbf{C}_{G_I}, \mathbf{C}_{G_{II}}, \cdots, \mathbf{C}_{G_N}\right), \mathbf{D}_G = diag\left(\mathbf{D}_{G_I}, \mathbf{D}_{G_{II}}, \cdots, \mathbf{D}_{G_N}\right) \end{aligned} \tag{16}$$

Using the sparsity patterns shown in (16), the controller in (14) is equivalent to multiple uncoupled controllers, each controller requiring only one group of feedback signals to determine the control forces for that group:

$$\begin{cases} \mathbf{x}_{G_I}[k+1] = \mathbf{A}_{G_I}\mathbf{x}_{G_I}[k] + \mathbf{B}_{G_I}\mathbf{y}_I[k] \\ \mathbf{u}_I[k] = \mathbf{C}_{G_I}\mathbf{x}_{G_I}[k] + \mathbf{D}_{G_I}\mathbf{y}_I[k] \end{cases}, \\ \cdots, \\ \begin{cases} \mathbf{x}_{G_N}[k+1] = \mathbf{A}_{G_N}\mathbf{x}_{G_N}[k] + \mathbf{B}_{G_N}\mathbf{y}_N[k] \\ \mathbf{u}_N[k] = \mathbf{C}_{G_N}\mathbf{x}_{G_N}[k] + \mathbf{D}_{G_N}\mathbf{y}_N[k] \end{cases} \tag{17}$$

As an example, for the feedback pattern with information overlapping shown in Fig. 2(b), the total number of groups, N, is equal to three and each control force group contains one entry; the feedback signals are aggregated as illustrated in Fig. 3, which shows that feedback signal group $\mathbf{y}_I[k]$ has four entries, $\mathbf{y}_{II}[k]$ has six entries, and $\mathbf{y}_{III}[k]$ has four entries.

Assuming that the $\mathbf{D}_{22}$ matrix in the open-loop system in (12) is a zero matrix, the following notations are defined [14]:

$$\left[\begin{array}{c|c|c} \tilde{\mathbf{A}} & \tilde{\mathbf{B}}_1 & \tilde{\mathbf{B}}_2 \\ \hline \tilde{\mathbf{C}}_1 & \tilde{\mathbf{D}}_{11} & \tilde{\mathbf{D}}_{12} \\ \hline \tilde{\mathbf{C}}_2 & \tilde{\mathbf{D}}_{21} & \end{array}\right] = \left[\begin{array}{cc|c|cc} \mathbf{A} & \mathbf{0} & \mathbf{B}_1 & \mathbf{0} & \mathbf{B}_2 \\ \mathbf{0} & \mathbf{0}_{n_G} & \mathbf{0} & \mathbf{I}_{n_G} & \mathbf{0} \\ \hline \mathbf{C}_1 & \mathbf{0} & \mathbf{D}_{11} & \mathbf{0} & \mathbf{D}_{12} \\ \hline \mathbf{0} & \mathbf{I}_{n_G} & \mathbf{0} & & \\ \mathbf{C}_2 & \mathbf{0} & \mathbf{D}_{21} & & \end{array}\right] \tag{18}$$

Zero submatrices with unspecified dimensions should have compatible dimensions with neighboring submatrices. Using the definitions above, the closed-loop system in Fig. 4 can be formulated by concatenating the open-loop system with the controller system:

$$\begin{cases} \mathbf{x}_{CL}[k+1] = \mathbf{A}_{CL}\mathbf{x}_{CL}[k] + \mathbf{B}_{CL}\mathbf{w}[k] \\ \mathbf{z}[k] = \mathbf{C}_{CL}\mathbf{x}_{CL}[k] + \mathbf{D}_{CL}\mathbf{w}[k] \end{cases} \tag{19}$$

where

$$\mathbf{A}_{CL} = \tilde{\mathbf{A}} + \tilde{\mathbf{B}}_2\mathbf{G}\tilde{\mathbf{C}}_2, \mathbf{B}_{CL} = \tilde{\mathbf{B}}_1 + \tilde{\mathbf{B}}_2\mathbf{G}\tilde{\mathbf{D}}_{21}, \\ \mathbf{C}_{CL} = \tilde{\mathbf{C}}_1 + \tilde{\mathbf{D}}_{12}\mathbf{G}\tilde{\mathbf{C}}_2, \mathbf{D}_{CL} = \tilde{\mathbf{D}}_{11} + \tilde{\mathbf{D}}_{12}\mathbf{G}\tilde{\mathbf{D}}_{21} \tag{20}$$

and **G** is defined in (15). Note that the input to the closed-loop system is **w**[*k*] defined in (13), and the output is the structural response **z**[*k*]. According to the Bounded Real Lemma, the following two statements are equivalent in specifying the performance criterion based on the $\mathcal{H}_\infty$ -norm [16]:

1. The $\mathcal{H}_\infty$ -norm of the closed-loop system in (19) is less than γ, and $\mathbf{A}_{CL}$ is stable in the discrete-time sense (*i.e.* all of the eigenvalues of $\mathbf{A}_{CL}$ fall in the unit circle on the complex plane);

2. There exists a symmetric positive definite matrix $\mathbf{P} > 0$ such that the following matrix inequality holds:

$$\begin{bmatrix} -\mathbf{P}^{-1} & \mathbf{A}_{CL} & \mathbf{B}_{CL} & \mathbf{0} \\ * & -\mathbf{P} & \mathbf{0} & \mathbf{C}_{CL}^T \\ * & * & -\gamma\mathbf{I} & \mathbf{D}_{CL}^T \\ * & * & * & -\gamma\mathbf{I} \end{bmatrix} < 0 \tag{21}$$

where * denotes a symmetric entry, and "< 0" means that the matrix at the left side of the inequality is negative definite. Pre and post-multiplying (21) by a positive definite matrix *diag*(**P**,**I**,**I**,**I**), the congruence transformation leads to the following matrix inequality:

$$\begin{bmatrix} -\mathbf{P} & \mathbf{P}\mathbf{A}_{CL} & \mathbf{P}\mathbf{B}_{CL} & \mathbf{0} \\ * & -\mathbf{P} & \mathbf{0} & \mathbf{C}_{CL}^T \\ * & * & -\gamma\mathbf{I} & \mathbf{D}_{CL}^T \\ * & * & * & -\gamma\mathbf{I} \end{bmatrix} < 0 \tag{22}$$

Substituting the definitions in (20) into (22), we define a matrix variable **F** which is a function of **G** and **P** as:

$$\mathbf{F}(\mathbf{G},\mathbf{P}) = \begin{bmatrix} -\mathbf{P} & \mathbf{P}\left(\tilde{\mathbf{A}} + \tilde{\mathbf{B}}_2\mathbf{G}\tilde{\mathbf{C}}_2\right) & \mathbf{P}\left(\tilde{\mathbf{B}}_1 + \tilde{\mathbf{B}}_2\mathbf{G}\tilde{\mathbf{D}}_{21}\right) & \mathbf{0} \\ * & -\mathbf{P} & \mathbf{0} & \left(\tilde{\mathbf{C}}_1 + \tilde{\mathbf{D}}_{12}\mathbf{G}\tilde{\mathbf{C}}_2\right)^T \\ * & * & -\gamma\mathbf{I} & \left(\tilde{\mathbf{D}}_{11} + \tilde{\mathbf{D}}_{12}\mathbf{G}\tilde{\mathbf{D}}_{21}\right)^T \\ * & * & * & -\gamma\mathbf{I} \end{bmatrix} \tag{23}$$

If there exists a decentralized controller **G** (with parameter structures illustrated in (16)), a positive real number γ, and a symmetric positive definite matrix **P**, such that **F**(**G**,**P**) < 0, then the closed-loop $\mathcal{H}_\infty$ -norm is less than γ. Because both **G** and **P** are unknown variables, the optimization problem has a bilinear matrix inequality (BMI) constraint [17]. When there is no sparsity requirements on the matrix **G**, efficient solvers are available for computing an ordinary controller matrix $\mathbf{G}_C$ that minimizes the closed-loop $\mathcal{H}_\infty$ -norm [16, 18]:

$$\mathbf{G}_C = \begin{bmatrix} \mathbf{A}_{G_C} & \mathbf{B}_{G_C} \\ \mathbf{C}_{G_C} & \mathbf{D}_{G_C} \end{bmatrix} \tag{24}$$

In general, $\mathbf{A}_{G_C}$, $\mathbf{B}_{G_C}$, $\mathbf{C}_{G_C}$, and $\mathbf{D}_{G_C}$ are full matrices that represent centralized information feedback. When sparsity patterns in the controller matrices are specified to achieve decentralized information feedback, off-the-shelf algorithms for solving the optimization problem with BMI constraints are not available [17]. In this study, a heuristic homotopy method for designing continuous-time decentralized controllers [14] is adapted for the discrete-time controller design. Starting with a centralized controller, the algorithm searches for a decentralized controller along following homotopy path:

$$\mathbf{G} = (1-\lambda)\mathbf{G}_C + \lambda\mathbf{G}_D, 0 \le \lambda \le 1 \tag{25}$$

where λ gradually increases from 0 to 1. $\mathbf{G}_C$ represents the initial centralized controller and $\mathbf{G}_D$ the desired decentralized controller. Assume that a total number of *M* steps are assigned for the homotopy path, and denote:

$$\lambda_k = k/M, k = 0,1,...,M \tag{26}$$

At every step *k* along the homotopy path, the two matrix variables $\mathbf{G}_D$ and **P** are held constant one at a time, so that only one variable needs to be solved every time. In this way, the BMI constraint in (23) degenerates into a linear matrix inequality (LMI) constraint. For convenience, a matrix variable **H** is defined based on (23) as a function of variables $\mathbf{G}_D$, **P**, and λ:

$$\mathbf{H}(\mathbf{G}_D,\mathbf{P},\lambda) = \mathbf{F}(\mathbf{G},\mathbf{P}) = \mathbf{F}\left((1-\lambda)\mathbf{G}_C + \lambda\mathbf{G}_D,\mathbf{P}\right) < 0 \tag{27}$$

Note that the centralized controller $\mathbf{G}_C$ is initially solved using any conventional methods and remains constant during the homotopy search.

At the beginning of a homotopy search, an upper bound for the closed-loop $\mathcal{H}_\infty$ -norm, i.e. γ, is specified. The unknown variables in the above matrix inequality consist of $\mathbf{G}_D$ and **P** only. When $\mathbf{G}_D$ is held constant, a new **P** matrix can be computed for the next step; on the other hand, when **P** is held constant, a new $\mathbf{G}_D$ matrix is computed. If a homotopy search fails, γ is increased by certain relaxation factor and a new search is conducted. The modified algorithm is described as follows:

[i] Compute a centralized controller $\mathbf{G}_C$ and the minimum closed-loop $\mathcal{H}_\infty$ -norm γ_C using existing robust control solvers [16, 18]; set $\gamma \leftarrow \gamma_C$, and set an upper limit ($\gamma_{\max}$) for γ, e.g. $10^6\gamma_C$.

[ii] Initialize *M*, the total number of homotopy steps, to be a positive number, e.g. 2^8, and set an upper limit ($M_{\max}$) for

M, e.g. 2^{13}; Set $k \leftarrow 0$, $\lambda_0 \leftarrow 0$, and $\mathbf{G}_{D0} \leftarrow \mathbf{0}$; compute a feasible solution $\mathbf{P}_0$ under the constraint $\mathbf{H}(\mathbf{G}_{D0}, \mathbf{P}_0, \lambda_0) < 0$.

[iii] Set $k \leftarrow k+1$, and $\lambda_k \leftarrow k/M$; compute a solution $\mathbf{G}_D$ under the constraint $\mathbf{H}(\mathbf{G}_D, \mathbf{P}_{k-1}, \lambda_k) < 0$. If it is not feasible, go to Step [iv]. If $\mathbf{H}(\mathbf{G}_D, \mathbf{P}_{k-1}, \lambda_k) < 0$ is feasible, set $\mathbf{G}_{Dk} \leftarrow \mathbf{G}_D$, and compute a solution $\mathbf{P}$ under the constraint $\mathbf{H}(\mathbf{G}_{D_k}, \mathbf{P}, \lambda_k) < 0$. If $\mathbf{H}(\mathbf{G}_{D_k}, \mathbf{P}, \lambda_k) < 0$ is feasible, set $\mathbf{P}_k \leftarrow \mathbf{P}$, and go to Step [v]; if not, go to Step [vi].

[iv] Compute a solution $\mathbf{P}$ for $\mathbf{H}(\mathbf{G}_{D_{k-1}}, \mathbf{P}, \lambda_k) < 0$. If $\mathbf{H}(\mathbf{G}_{D_{k-1}}, \mathbf{P}, \lambda_k) < 0$ is not feasible, go to Step [vi]. If it is feasible, set $\mathbf{P}_k \leftarrow \mathbf{P}$ and compute a solution $\mathbf{G}_D$ under the constraint $\mathbf{H}(\mathbf{G}_D, \mathbf{P}_k, \lambda_k) < 0$. If $\mathbf{H}(\mathbf{G}_D, \mathbf{P}_k, \lambda_k) < 0$ is feasible, set $\mathbf{G}_{Dk} \leftarrow \mathbf{G}_D$ and go to Step [v]; if not, go to Step [vi].

[v] If $k < M$, go to Step [iii]. If k is equal to M, $\mathbf{G}_{Dk}$ is the solution of the decentralized control problem.

[vi] Set $M \leftarrow 2M$ under the constraint $M \le M_{\max}$ and restart the searching from Step [ii]. If M reaches over $M_{\max}$, set $\gamma \leftarrow s_\gamma \gamma$ (s_γ is a relaxation factor that is greater than one) under the constraint $\gamma \le \gamma_{\max}$ and restart from Step [ii]. If γ reaches over $\gamma_{\max}$, it is concluded that the computation doesn't converge.

A decentralized controller is found when k is equal to M at step [v]. The controller has the property that the closed-loop $\mathcal{H}_\infty$ -norm is less than γ. It should be pointed out that since the homotopy algorithm is heuristic in nature, non-convergence in the computation does not imply that the decentralized $\mathcal{H}_\infty$ control problem has no solution.

IV. Numerical Example

This section first illustrates procedures of the decentralized $\mathcal{H}_\infty$ controller design using a three-story example structure. Performance of the decentralized $\mathcal{H}_\infty$ controllers is then presented.

A. Formulation of the Three-story Example Structure

As shown in Fig. 1, the three-story building is modeled as an in-plane lumped-mass structure with one control device allocated between every two neighboring floors. The mass, stiffness, and damping matrices are given as:

$$\mathbf{M} = \begin{bmatrix} 6 & & \\ & 6 & \\ & & 6 \end{bmatrix} \times 10^3 \text{ kg}, \mathbf{K} = \begin{bmatrix} 3.4 & -1.8 & \\ -1.8 & 3.4 & -1.6 \\ & -1.6 & 1.6 \end{bmatrix} \times 10^6 \text{ N/m},$$
$$\mathbf{C} = \begin{bmatrix} 12.4 & -5.16 & \\ -5.16 & 12.4 & -4.59 \\ & -4.59 & 7.20 \end{bmatrix} \times 10^3 \text{ N/(m/s)} \quad (28)$$

A discrete-time system describing the structural dynamics is given in (9). Considering inter-story drifts as the control parameters, the output matrices are defined as follows:

$$\mathbf{C}_\mathbf{z} = \begin{bmatrix} 1 & 0 & 0 & 0 & 0 & 0 \\ -1 & 0 & 1 & 0 & 0 & 0 \\ 0 & 0 & -1 & 0 & 1 & 0 \\ 0 & 0 & 0 & 0 & 0 & 0 \\ 0 & 0 & 0 & 0 & 0 & 0 \\ 0 & 0 & 0 & 0 & 0 & 0 \end{bmatrix}, \mathbf{F}_\mathbf{z} = \mathbf{0}, \mathbf{D}_\mathbf{z} = \begin{bmatrix} 0 & 0 & 0 \\ 0 & 0 & 0 \\ 0 & 0 & 0 \\ 1 & 0 & 0 \\ 0 & 1 & 0 \\ 0 & 0 & 1 \end{bmatrix} \times 10^{-6} \quad (29)$$

With $\mathbf{C}_\mathbf{z}$ and $\mathbf{D}_\mathbf{z}$ defined above, the 2-norm of the output vector $\mathbf{z}[k]$ becomes a quadratic function of the inter-story drifts and the control forces:

$$\begin{aligned} \|\mathbf{z}[k]\|_2^2 &= \|\mathbf{C}_\mathbf{z}\mathbf{x}_S[k] + \mathbf{D}_\mathbf{z}\mathbf{u}[k]\|_2^2 \\ &= \left[q_1^2[k] + (q_2[k] - q_1[k])^2 + (q_3[k] - q_2[k])^2 \right] + \\ &\quad 10^{-12}\left(u_1^2[k] + u_2^2[k] + u_3^2[k]\right) \end{aligned} \quad (30)$$

where $q_i[k]$ and $u_i[k]$ represent, respectively, the floor displacement relative to the ground and the control force for floor i. The relative weighting between the structural response and the control effort is reflected by the magnitude of matrices $\mathbf{C}_\mathbf{z}$ and $\mathbf{D}_\mathbf{z}$.

It is assumed that inter-story drifts and velocities can be measured, i.e. the measurement vector $\mathbf{m}[k]$ is defined as $\{ q_1[k],\ \dot{q}_1[k],\ q_2[k]-q_1[k],\ \dot{q}_2[k]-\dot{q}_1[k],\ q_3[k]-q_2[k],\ \dot{q}_3[k]-\dot{q}_2[k] \}^{\mathrm{T}}$. Hence, the measurement matrices in (9) are determined as:

$$\mathbf{C}_\mathbf{m} = \begin{bmatrix} 1 & 0 & 0 & 0 & 0 & 0 \\ 0 & 1 & 0 & 0 & 0 & 0 \\ -1 & 0 & 1 & 0 & 0 & 0 \\ 0 & -1 & 0 & 1 & 0 & 0 \\ 0 & 0 & -1 & 0 & 1 & 0 \\ 0 & 0 & 0 & -1 & 0 & 1 \end{bmatrix}, \ \mathbf{F}_\mathbf{m} = \mathbf{0}, \ \mathbf{D}_\mathbf{m} = \mathbf{0} \quad (31)$$

B. Controller Designs with Different Feedback Patterns

Controllers are designed for three different feedback patterns: fully decentralized, partially decentralized, and centralized. The two decentralized feedback patterns follow the schematics in Fig. 2. For example, in the fully decentralized case, only two sensor measurements (i.e. the inter-story drift and velocity) are available for the sub-controller at each story. In the centralized feedback case, all six measurements at three stories are available while making control decisions for each control device. As shown in Table 1, each feedback pattern is identified by a degree-of-centralization (DC). For the partially decentralized pattern with information overlapping, the feedback signal is re-defined as shown in Fig. 3. A sampling period of 5ms is first used for the results presented below; this implies that the feedback time delay is also set as 5ms.

Table 1 Three Feedback Patterns

Degrees of Centralization (DC)	DC ①	DC ②	DC ③
Description	Fully decentralized (Fig. 2a)	Partially decentralized (Fig. 2b)	Centralized

The homotopy method is used to compute the time-delayed decentralized control solutions. For the fully decentralized case DC ①, each uncoupled controller, $\mathbf{G}_I^{①}$, $\mathbf{G}_{II}^{①}$, or $\mathbf{G}_{III}^{①}$. takes two feedback signals as input (i.e. inter-story drift and velocity at the story housing the decentralized controller), and outputs the desired control force at this story. For example, the decentralized controller $\mathbf{G}_I^{①}$ determined by the homotopy search has 2 input variables, 4 state variables, and 1 output variable. For the partially decentralized case DC ②, three uncoupled decentralized controllers are computed as well, where the dimensions of the three controllers are summarized in Table 2. For case DC ③, the centralized controller has 6 input variables (inter-story drifts and velocities at all stories), 12 state variables, and 3 output variables (control forces).

Table 3 shows the open-loop $\mathcal{H}_\infty$ -norm of the uncontrolled structure, as well as the closed-loop $\mathcal{H}_\infty$ -norms of the controlled structure. Compared with the three controlled cases, the uncontrolled structure has a much higher $\mathcal{H}_\infty$ -norm, which indicates larger worst-case amplification from the disturbance **w** to the output **z**. Among the three controlled cases, the centralized controller assumes that complete state information is available for control decisions of all three control devices; accordingly, the centralized controller achieves the minimum closed-loop $\mathcal{H}_\infty$ -norm (which means best $\mathcal{H}_\infty$ performance). The fully decentralized control case achieves the largest closed-loop norm among the three controlled cases, as the least amount of information is available for control decisions. It can be seen that, even with 5ms of time delay in the feedback loop, all three controlled cases achieve smaller closed-loop $\mathcal{H}_\infty$ norms than the uncontrolled structure.

C. Simulation Results

One ideal actuator that generates arbitrary desired control force is deployed at each story of the structure. The 1940 El Centro NS (Imperial Valley Irrigation District Station) earthquake record with its peak acceleration scaled to 2m/s^2 is used as the ground excitation. As described in the last subsection, decentralized/centralized controllers considering 5ms of feedback delay are designed for the three feedback patterns (DC ①, DC ②, and DC ③). To improve the simulation accuracy, regardless of the feedback time delay or sampling time period, a time step of 1ms is used in the dynamic simulation. Simulated inter-story drifts at all three stories are plotted in Fig. 5. For clarity, the plots are zoomed in to the part when peak drifts occur. Also presented are the inter-story drifts of the uncontrolled structure. As shown in the figure, although 5ms of feedback time delay exists, all three feedback control cases achieve significant reduction in the inter-story drifts. No control instability is observed even though the actuators can generate arbitrarily large forces.

Table 2 Dimensions of Decentralized Controllers for Pattern DC ②

Number of variables	$\mathbf{G}_I^{②}$	$\mathbf{G}_{II}^{②}$	$\mathbf{G}_{III}^{②}$
Input	4	6	4
State	4	4	4
Output	1	1	1

Table 3 $\mathcal{H}_\infty$ -norms of Uncontrolled and Controlled Structures

	Uncontrolled	DC ①	DC ②	DC ③
$\|\mathbf{H}_{zw}\|_\infty$	0.1688	0.06113	0.02419	0.02348

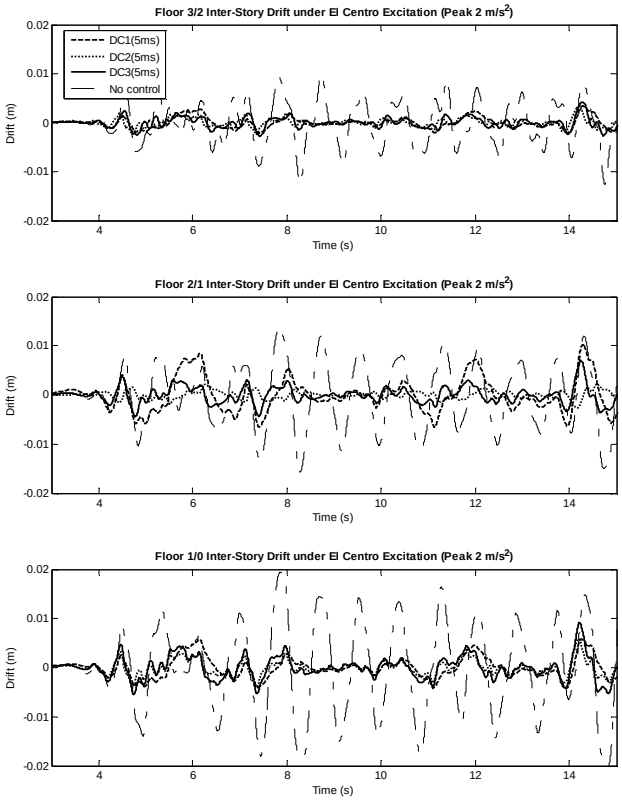

Fig. 5. Inter-story drifts of the three-story structure (time delay is 5ms).

Fig. 6 presents the peak inter-story drifts at the three stories, and the peak actuator forces required by the three different control cases. As shown in Fig. 6(a), the partially decentralized case, DC ②, achieves the least overall peak inter-story drifts among the three feedback patterns. The fully decentralized case, DC ①, achieves small peak drifts at the first and the third story, but has the highest peak drift at the second story. The centralized case, DC ③, results in higher drifts at all three stories, when compared with case DC ②. The better performance of case DC ② on reducing inter-story drifts is partly attributed to its higher requirement on peak actuator forces. As shown in Fig. 6(b), case DC ② requires higher peak actuator forces than the other two cases.

To illustrate the effect of different time delays due to different degrees of decentralization, additional simulations are conducted with different time delays adopted for three different feedback patterns. For case DC ①, where each actuator only requires sensor data at its own story to make control decisions, time delay is chosen to be the minimum as 5ms. For case DC ②, where data from sensors on the actuator's own story and neighboring story (stories) are required, 10ms time delay is adopted. For the centralized case

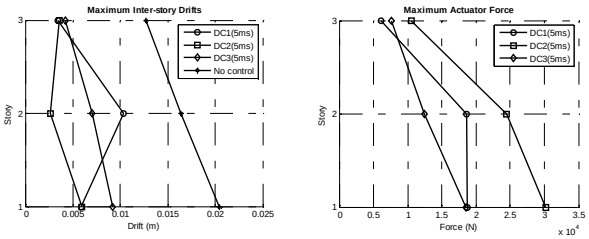

(a) (b)

Fig. 6. Peak inter-story drifts and actuator forces when ideal actuators are deployed on the three-story structure; time delay of 5ms is adopted for all three feedback patterns.

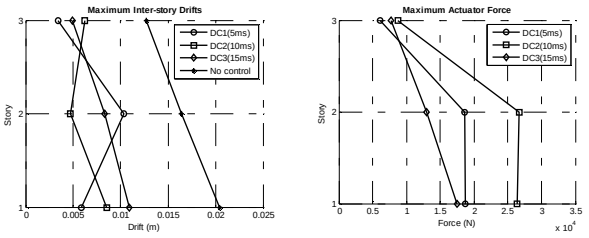

(a) (b)

Fig. 7. Peak inter-story drifts and actuator forces when ideal actuators are deployed on the three-story structure; different time delays are adopted for different feedback patterns.

DC ③ , 15ms time delay is adopted. For feedback patterns DC ② and DC ③ , controllers are re-computed based on the different time delays. Simulated peak inter-story drifts and actuator forces are presented in Fig. 7. A comparison between Fig. 7(a) and Fig. 6(a) shows that due to longer time delay, the performance of cases DC ② and DC ③ degrades. Among the three feedback cases shown in Fig. 7(a), the partially decentralized case DC ② offers the most preferable performance in terms of reducing peak inter-story drifts. Fig. 7(b) illustrates that case DC ② again requires the highest peak actuator forces. The peak floor accelerations achieved by DC ② are comparable with DC ③ ; both these two cases achieve slightly larger peak accelerations than DC ① .

V. Conclusion

This paper presents a decentralized controller design that aims to minimize the closed-loop $\mathcal{H}_\infty$ norm of a controlled structure. The design is formulated in discrete-time domain, and considers possible feedback time delay. The decentralized controller design employs a homotopy method, which gradually degenerates a centralized controller into a set of uncoupled decentralized controllers. LMI constraints describing the closed-loop $\mathcal{H}_\infty$ norm performance are ensured at each homotopy step. Performance of the decentralized $\mathcal{H}_\infty$ controller design is validated through numerical simulations. It is illustrated that decentralized control strategies may provide equivalent or even better control performance, given that their centralized counterparts could suffer longer sampling periods due to communication and computation constraints.

Acknowledgment

This work was partially supported by NSF, Grant Number CMMI-0824977, awarded to Prof. Kincho H. Law of Stanford University. The authors appreciate the insightful opinions on this research from Prof. Jerome P. Lynch of the University of Michigan. The authors would also like to thank Prof. Chin-Hsiung Loh of the National Taiwan University for sharing the 3-story structure model built at the National Center for Research on Earthquake Engineering in Taiwan.

References

[1] T. T. Soong, *Active Structural Control: Theory and Practice*. Harlow, Essex, England: Wiley, 1990.

[2] B. F. Spencer, Jr. and S. Nagarajaiah, "State of the art of structural control," *Journal of Structural Engineering*, vol. 129, pp. 845-856, 2003.

[3] Y. Wang, R. A. Swartz, J. P. Lynch, K. H. Law, K.-C. Lu, and C.-H. Loh, "Decentralized civil structural control using real-time wireless sensing and embedded computing," *Smart Structures and Systems*, vol. 3, pp. 321-340, 2007.

[4] J. P. Lynch, Y. Wang, R. A. Swartz, K.-C. Lu, and C.-H. Loh, "Implementation of a closed-loop structural control system using wireless sensor networks," *Structural Control and Health Monitoring*, vol. 15, pp. 518-539, 2008.

[5] J. P. Lynch and D. M. Tilbury, "Implementation of a decentralized control algorithm embedded within a wireless active sensor," in *Proceedings of the 2nd Annual ANCRiSST Workshop*, Gyeongju, Korea, 2005.

[6] D. D. Siljak, *Decentralized Control of Complex Systems*. Boston: Academic Press, 1991.

[7] J. G. Chase and H. A. Smith, "Robust H_∞ control considering actuator saturation. I: theory," *Journal of Engineering Mechanics*, vol. 122, pp. 976-983, 1996.

[8] C.-C. Lin, C.-C. Chang, and H.-L. Chen, "Optimal H_∞ output feedback control systems with time delay," *Journal of Engineering Mechanics*, vol. 132, pp. 1096-1105, 2006.

[9] E. A. Johnson, P. G. Voulgaris, and L. A. Bergman, "Multiobjective optimal structural control of the Notre Dame building model benchmark," *Earthquake Engineering & Structural Dynamics*, vol. 27, pp. 1165-1187, 1998.

[10] J. N. Yang, S. Lin, and F. Jabbari, "H_∞-based control strategies for civil engineering structures," *Structural Control and Health Monitoring*, vol. 11, pp. 223-237, 2004.

[11] J. G. Chase, H. A. Smith, and T. Suzuki, "Robust H_∞ control considering actuator saturation. II: applications," *Journal of Engineering Mechanics*, vol. 122, pp. 984-993, 1996.

[12] S. Boyd, L. El Ghaoui, E. Feron, and V. Balakrishnan, *Linear Matrix Inequalities in System and Control Theory*. Philadelphia, PA: SIAM, 1994.

[13] Y. Wang, J. P. Lynch, and K. H. Law, "Decentralized H_∞ controller design for large-scale wireless structural sensing and control systems," in *Proceedings of the 6th International Workshop on Structural Health Monitoring*, Stanford, CA, 2007.

[14] G. Zhai, M. Ikeda, and Y. Fujisaki, "Decentralized H_∞ controller design: a matrix inequality approach using a homotopy method," *Automatica*, vol. 37, pp. 565-572, 2001.

[15] S. Y. Chu, T. T. Soong, and A. M. Reinhorn, *Active, Hybrid, and Semi-active Structural Control: a Design and Implementation Handbook*. Hoboken, NJ: Wiley, 2005.

[16] P. Gahinet and P. Apkarian, "A linear matrix inequality approach to H_∞ control," *International Journal of Robust and Nonlinear Control*, vol. 4, pp. 421-448, 1994.

[17] J. G. VanAntwerp and R. D. Braatz, "A tutorial on linear and bilinear matrix inequalities," *Journal of Process Control*, vol. 10, pp. 363-385, 2000.

[18] R. Y. Chiang and M. G. Safonov, *MATLAB robust control toolbox*, 2 ed. Natick, MA: MathWorks, Inc., 1998.